J|A|C|S ARTICLES

Published on Web 11/22/2010

Bodipy Dyes with Tunable Redox Potentials and Functional Groups for Further Tethering: Preparation, Electrochemical, and Spectroscopic Characterization

Katerina Krumova and Gonzalo Cosa*

Department of Chemistry and Center for Self Assembled Chemical Structures (CSACS/CRMAA), McGill University, 801 Sherbrooke Street West, Montreal, Quebec H3A 2K6, Canada

Received August 21, 2010; E-mail: gonzalo.cosa@mcgill.ca

Abstract: The preparation, spectroscopic, and electrochemical characterization of a family of 16 new bodipy dyes with tunable redox potentials and versatile functional groups is reported. Electron-withdrawing or -donating groups (Et, H, Cl, or CN) at positions C2 and C6 enabled tuning the redox potentials within a ca. 0.7 eV window without significantly affecting either the HOMO−LUMO gap or the absorption and emission spectra. Hydroxymethyl or formyl groups at the meso (C8) position in turn provided a handle for covalent tethering to receptors and biomolecules of interest, which dispenses with the more commonly used *meso*-aryl moiety as a means to tag molecules. The dyes can thus be coupled to both electrophiles and nucleophiles. Importantly, it is shown that *meso*-formyl bodipy dyes are nonemissive and have significantly lower molar extinction coefficients compared to their *meso*-hydroxymethyl and *meso*-acetoxymethyl counterparts (which in turn are bright, with emission quantum yields in the range of 0.7−1). The nonemissive *meso*-formyl bodipy dyes thus provide unique opportunities as fluorogenic probes of nucleophilic attack and as fluorescent labeling agents where uncoupled fluorophores will not contribute to the fluorescence background. Overall, the new bodipy dyes reported here are promising candidates for the preparation of fluorescent sensors relying on photoinduced electron transfer and may find use in a number of fluorescent-labeling protocols.

Introduction

Following the first report in 1968, boron dipyrromethene or bodipy dyes[1] have been increasingly adopted for various different fluorescence imaging applications.[2,3] To a great extent bodipy dyes owe popularity to their relative ease of preparation[4,5] and optimal spectroscopic properties (high emission quantum yields, high extinction coefficients, and narrow absorption and emission bands).[6,7] Bodipy dyes have been utilized, among others, as fluorescent positional tags in the form of lipid membrane markers in model membranes[3,8] or live cells,[9,10] as donor or acceptor fluorophores in FRET schemes to probe conformational rearrangements in biomolecules,[11] and as sensors/analyte indicators of ions[12] or reactive oxygen and nitrogen species.[9,13−15]

In the case of sensors/analyte indicators, most bodipy-based probes described rely on the action of an intramolecular off−on switch based on a photoinduced electron transfer (PeT) mechanism (receptor−reporter probes).[16,17] Tuning the redox potentials of the bodipy dyes, in order that PeT processes are thermodynamically feasible, is thus of primary importance in designing and developing novel sensors. It is important to emphasize that introducing new functional groups for highly

(1) Alfred, T.; Franz-Heinrich, K. *Justus Liebigs Ann. Chem.* **1968**, *718*, 208–223.
(2) Haugland, R. P. *Handbook of Fluorescent Probes and Research Products*, 10th ed.; Molecular Probes, Inc.: Eugene, OR, 2005.
(3) Johnson, I. D.; Kang, H. C.; Haugland, R. P. *Anal. Biochem.* **1991**, *198*, 228–237.
(4) (a) Loudet, A.; Burgess, K. *Chem. Rev.* **2007**, *107*, 4891–4932. (b) Gilles, U.; Raymond, Z.; Anthony, H. *Angew. Chem., Int. Ed.* **2008**, *47*, 1184–1201.
(5) Wood, T. E.; Thompson, A. *Chem. Rev.* **2007**, *107*, 1831–1861.
(6) (a) Ziessel, R.; Ulrich, G.; Harriman, A. *New J. Chem.* **2007**, *31*, 496–501. (b) Qin, W.; Rohand, T.; Dehaen, W.; Clifford, J. N.; Driesen, K.; Beljonne, D.; Van Averbeke, B.; Van der Auweraer, M.; Boens, N. l. *J. Phys. Chem. A* **2007**, *111*, 8588–8597. (c) Qin, W.; Baruah, M.; Van der Auweraer, M.; De Schryver, F. C.; Boens, N. l. *J. Phys. Chem. A* **2005**, *109*, 7371–7384.
(7) Arbeloa, F. L. p.; Bañuelos, J.; Martínez, V.; Arbeloa, T.; Arbeloa, I. L. p. *Int. Rev. Phys. Chem.* **2005**, *24*, 339–374.
(8) Korlach, J.; Schwille, P.; Webb, W. W.; Feigenson, G. W. *Proc. Natl. Acad. Sci. U.S.A.* **1999**, *96*, 8461–8466.
(9) (a) Drummen, G. P. C.; van Liebergen, L. C. M.; Op den Kamp, J. A. F.; Post, J. A. *Free Radical Biol. Med.* **2002**, *33*, 473–490. (b) Pap, E. H. W.; Drummen, G. P. C.; Winter, V. J.; Kooij, T. W. A.; Rijken, P.; Wirtz, K. W. A.; Op den Kamp, J. A. F.; Hage, W. J.; Post, J. A. *FEBS Lett.* **1999**, *453*, 278–282.
(10) Lemcke, S.; Hönnscheidt, C.; Waschatko, G.; Bopp, A.; Lütjohann, D.; Bertram, N.; Gehrig-Burger, K. *Mol. Cell. Endocrinol.* **2010**, *314*, 31–40.
(11) (a) Singh, K. K.; Parwaresch, R.; Krupp, G. *RNA* **1999**, *5*, 1348–1356. (b) Danell, A. S.; Parks, J. H. *Int. J. Mass Spectrom.* **2003**, *229*, 35–45.
(12) (a) Zeng, L.; Miller, E. W.; Pralle, A.; Isacoff, E. Y.; Chang, C. J. *J. Am. Chem. Soc.* **2005**, *128*, 10–11. (b) Yuan, M.; Li, Y.; Li, J.; Li, C.; Liu, X.; Lv, J.; Xu, J.; Liu, H.; Wang, S.; Zhu, D. *Org. Lett.* **2007**, *9*, 2313–2316. (c) Wang, J.; Qian, X. *Org. Lett.* **2006**, *8*, 3721–3724. (d) Baruah, M.; Qin, W.; Vallee, R. A. L.; Beljonne, D.; Rohand, T.; Dehaen, W.; Boens, N. *Org. Lett.* **2005**, *7*, 4377–4380. (e) Bozdemir, O. A.; Sozmen, F.; Buyukcakir, O.; Guliyev, R.; Cakmak, Y.; Akkaya, E. U. *Org. Lett.* **2010**, *12*, 1400–1403. (f) Peng, X.; Du, J.; Fan, J.; Wang, J.; Wu, Y.; Zhao, J.; Sun, S.; Xu, T. *J. Am. Chem. Soc.* **2007**, *129*, 1500–1501.
(13) Krumova, K.; Oleynik, P.; Karam, P.; Cosa, G. *J. Org. Chem.* **2009**, *74*, 3641–3651.

10.1021/ja1075663

	R^1	R^2
PM605	Et	Et
1	H	H
2	H	Cl
3	Cl	Cl
4	H	CN
5	CN	CN

	R^1	R^2
PMOH	Et	Et
6	H	H
7	H	Cl
8	Cl	Cl
9	H	CN
10	CN	CN

	R^1	R^2
11	Et	Et
12	H	H
13	H	Cl
14	Cl	Cl
15	H	CN
16	CN	CN

Figure 1. Structure of the bodipy dyes prepared and characterized in this work (**1**−**16**). Also shown are the structures of the commercially available dye PM605 and its derivative PMOH. Positions 2, 6, and 8 (meso) are shown in green.[5]

versatile tethering is critical in designing new bodipy dyes in order to enable their tagging to receptors and to other molecules of interest.

Here we describe the preparation, electrochemical, and spectroscopic characterization of a series of new bodipy dyes (see Figure 1). These dyes contain electron-donating or -withdrawing groups including Et, H, Cl, and CN at positions C2 and C6 of the backbone, enabling tuning of the redox potential within a 0.7 eV window. The meso position is functionalized with a hydroxymethyl or formyl group for further tethering. The rationale for this design is (i) to provide a suitable functional group to tether molecules of interest, where our criteria is to minimize the distance between the bodipy dye (reporter) and a covalently linked receptor in order to facilitate photoinduced electron transfer processes[18] in receptor−reporter systems, and (ii) to dispense with the use of a *meso*-aryl moiety as a handle to tether molecules of interest. Whereas a *meso*-aryl moiety is currently the preferred method to introduce a handle on bodipy dyes, it enhances the nonradiative excited state deactivation via internal conversion processes arising from rotation along the bond connecting the aryl moiety and the boron dipyrromethene backbone.[19] The aryl moiety may further insulate the dye (reporter) from a receptor segment in receptor−reporter probes, since typically the bodipy plane and that of the meso aromatic moiety lie at 90° with respect to each other (propeller like) and are thus conjugatively uncoupled.[15,20]

Results and Discussion

In the following section we first describe the preparation of the new bodipy dyes, and subsequently, we discuss their photophysical properties and electrochemical potentials.

Preparation of Bodipy Dyes. Bodipy dyes are usually synthesized by the condensation reaction between a carbonyl (either acyl chlorides or aromatic aldehydes) and a pyrrole followed by in situ complexation with $BF_3 \cdot OEt_2$ in the presence of a base.[5] We identified the condensation between substituted pyrroles and acetoxyacetyl chloride[21] (see Schemes 1 and 2) as the preferred method to prepare the bodipy dyes described here. Precursor pyrroles bearing either electron-withdrawing or -donating groups at the C3 position were utilized; this translated to C2 and C6 substitution in the resulting bodipy dyes. Whereas this substitution had only a minor effect on the HOMO−LUMO gap of these dyes (ranging between 2.26 and 2.42 eV), it had a dramatic effect on their redox potentials which spanned over 0.7 eV (see below). The condensation also allowed us to introduce the acetoxy group at the meso position which could be then converted first to a *meso*-hydroxymethyl bodipy (**6**−**10**) upon ester hydrolysis and, via subsequent oxidation, to a *meso*-formyl bodipy (**11**−**16**). New dyes were thus obtained with diverse electrochemical properties and versatile tethering potential.

Compound **1** was synthesized in two steps in 75% overall yield by condensation of acetoxyacetyl chloride and 2 equiv of 2,4-dimethyl pyrrole under reflux in dichloromethane followed by treatment of the reaction mixture with 4 equiv of $BF_3 \cdot OEt_2$ and diisopropylethylamine at room temperature.

Chlorination of compound **1** using *N*-chlorosuccinimide[22] afforded either compound **2** (Scheme 2) or **3** (Scheme 1) depending on the reaction conditions. Compound **2** was obtained in 76% yield after 12 h of reaction. Leaving the reaction for 36 h gave compound **3** in 92% yield, where additional reaction time was necessary due to deactivation of the aromatic system upon introduction of the first chlorine atom. Compound **5** was prepared in 30% overall yield via condensation of 3-cyano-2,4-dimethyl pyrrole (**17**, prepared following a modified literature procedure[17,23]) with acetoxyacetyl chloride followed by addition of diisopropylethylamine and 4 equiv of $BF_3 \cdot OEt_2$ (Scheme 1). Extended heating was required during condensation due to the lower nucleophilicity of **17**.

Asymmetric bodipy dyes are usually prepared by condensation of 2-formyl-pyrroles with a second pyrrole bearing a free α position.[5] This procedure however does not allow for introduction of a handle at the meso position.

We envisioned that using 2-ketopyrrole (**18**) as a precursor would provide us with a necessary handle. In order to prepare this compound, we exploited the low reactivity of **17** in its condensation with acetoxyacetylchloride, which allowed us to stop the reaction at the formation of **18** (see Scheme 2). The

(14) (a) Oleynik, P.; Ishihara, Y.; Cosa, G. *J. Am. Chem. Soc.* **2007**, *129*, 1842–1843. (b) Khatchadourian, A.; Krumova, K.; Boridy, S.; Ngo, A. T.; Maysinger, D.; Cosa, G. *Biochemistry* **2009**, *48*, 5658–5668. (c) Gabe, Y.; Ueno, T.; Urano, Y.; Kojima, H.; Nagano, T. *Anal. Bioanal. Chem.* **2006**, *386*, 621–626. (d) Yasuyuki, Y.; Yumiko, T.; Akinori, M.; Masahiko, I.; Shin, A. *ChemBioChem* **2008**, *9*, 853–856. (e) Sun, Z.-N.; Wang, H.-L.; Liu, F.-Q.; Chen, Y.; Tam, P. K. H.; Yang, D. *Org. Lett.* **2009**, *11*, 1887–1890. (f) Andrew, C. B.; Graeme, C.; Kristopher, J. E.; Ross, W. H.; William, C. *Eur. J. Org. Chem.* **2008**, *2008*, 2705–2713. (g) Sun, Z.-N.; Liu, F.-Q.; Chen, Y.; Tam, P. K. H.; Yang, D. *Org. Lett.* **2008**, *10*, 2171–2174.

(15) Gabe, Y.; Urano, Y.; Kikuchi, K.; Kojima, H.; Nagano, T. *J. Am. Chem. Soc.* **2004**, *126*, 3357–3367.

(16) (a) de Silva, A. P.; Gunaratne, H. Q. N.; Gunnlaugsson, T.; Huxley, A. J. M.; McCoy, C. P.; Rademacher, J. T.; Rice, T. E. *Chem. Rev.* **1997**, *97*, 1515–1566. (b) Ueno, T.; Urano, Y.; Setsukinai, K.; Takakusa, H.; Kojima, H.; Kikuchi, K.; Ohkubo, K.; Fukuzumi, S.; Nagano, T. *J. Am. Chem. Soc.* **2004**, *126*, 14079–14085.

(17) Ueno, T.; Urano, Y.; Kojima, H.; Nagano, T. *J. Am. Chem. Soc.* **2006**, *128*, 10640–10641.

(18) Turro, N. J.; Ramamurthy, V.; Scaiano, J. C. *Modern Molecular Photochemistry of Organic Molecules*; University Science Books: Sausalito, CA, 2010.

(19) (a) Kim, H.; Burghart, A.; Welch, M. B.; Reibenspies, J.; Burgess, K. *Chem. Commun.* **1999**, 1889–1890. (b) Thoresen, L. H.; Kim, H.; Welch, M. B.; Burghart, A.; Burgess, K. *Synlett* **1998**, *1998*, 1276–1278. (c) Prieto, J. B.; Arbeloa, F. L.; Martínez, V. M.; López, T. A.; Amat-Guerri, F.; Liras, M.; Arbeloa, I. L. *Chem. Phys. Lett.* **2004**, *385*, 29–35.

(20) Kollmannsberger, M.; Gareis, T.; Heinl, S.; Daub, J.; Breu, J. *Angew. Chem., Int. Ed.* **1997**, *36*, 1333–1335.

(21) Amat-Guerri, F.; Liras, M.; Carrascoso, M. L.; Sastre, R. *Photochem. Photobiol.* **2003**, *77*, 577–584.

(22) Li, L.; Nguyen, B.; Burgess, K. *Bioorg. Med. Chem. Lett.* **2008**, *18*, 3112–3116.

(23) Alberola, A.; González Ortega, A.; Luisa Sádaba, M.; Sañudo, C. *Tetrahedron* **1999**, *55*, 6555–6566.

Scheme 1. Synthesis of Symmetric Bodipy Dyes

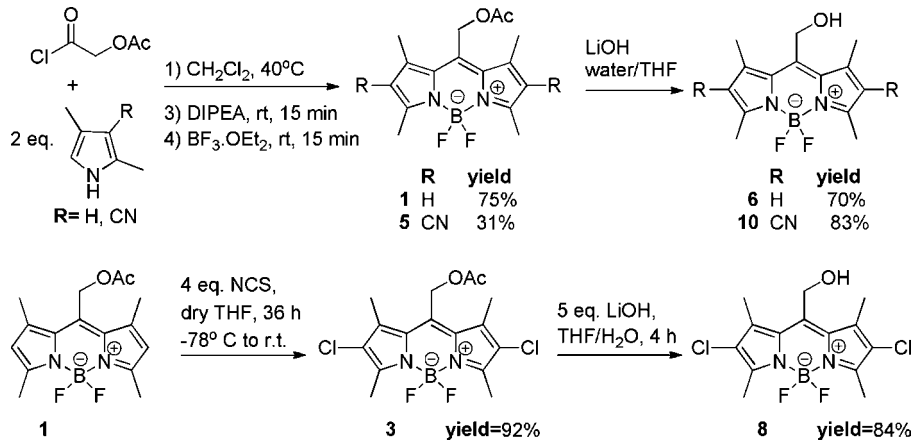

Scheme 2. Synthesis of Asymmetric Bodipy Dyes

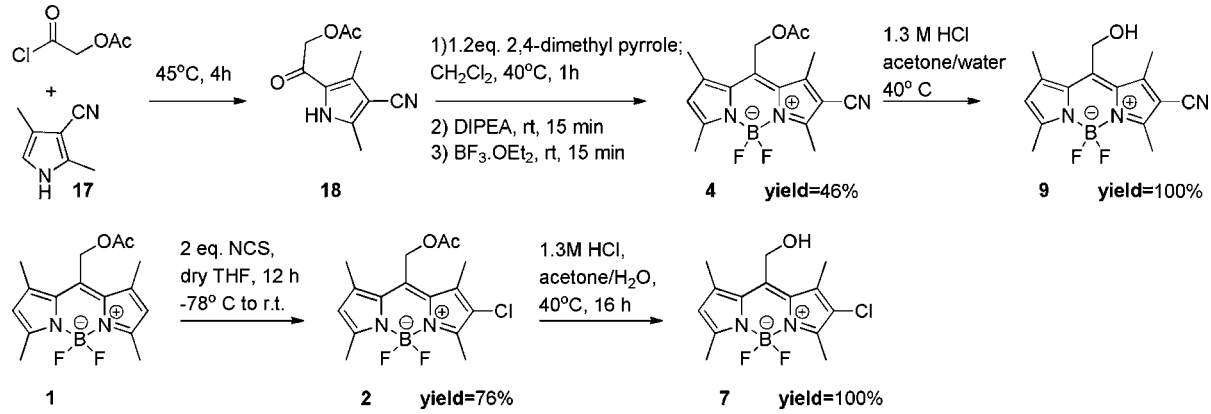

latter was next coupled with the more reactive 2,4-dimethyl pyrrole. After 1 h of reflux the reaction was cooled to room temperature; upon 10-fold dilution[24] and addition of an excess of DIPEA and $BF_3 \cdot OEt_2$ we obtained compound **4** in 46% yield (see Scheme 2).

The *meso*-acetoxymethyl bodipy derivatives **1**−**5** were easily hydrolyzed to the corresponding *meso*-hydroxymethyl bodipy **6**−**10** under basic or acidic conditions. Specifically, for the symmetric compounds **1**, **3**, and **5** hydrolysis was performed in basic media.[21]

It is interesting to note that when performing the basic hydrolysis of compounds **3** and **5** discoloration and loss of fluorescence occurred upon addition of the aqueous solution of LiOH to the solution of the dyes in THF, yet discoloration was not observed in the hydrolysis of compound **1**. Notably, the discoloration we observed in **3** and **5** was reversed when acidifying the solution following addition of 3 M HCl. The solution turned orange-pink, and compounds **8** and **10** were isolated in 80% and 83% yields, respectively. It is worth mentioning that discoloration has also been observed for other nitrile-substituted bodipy dyes.[25] In all cases these changes occurred under significantly milder conditions than those we employed in the hydrolysis of **3** and **5**.[25,26] Discoloration was not reversible, but it was pH sensitive.[25]

Basic hydrolysis of compounds **2** and **4** was initially attempted under identical conditions to those employed for the hydrolysis of **1**, **3**, and **5**, yet it did not lead to formation of the desired *meso*-hydroxymethyl bodipy dyes but rather resulted in decomposition of the dye and generation of secondary fluorescent products. The hydrolysis of compounds **2** and **4** was ultimately accomplished under acidic conditions (1.3 M HCl in acetone, 40 °C),[21] affording the alcohol in quantitative yield after 3 and 16 h of reaction, respectively. No change in either absorption or emission occurred under these hydrolysis conditions. These conditions however led to decomposition of the symmetric bodipy dyes PM605 and **1**, **3**, and **5**.

Oxidation of PMOH and compounds **6**−**10** to the corresponding *meso*-formyl bodipy (compounds **11**−**16**) was done using standard Dess−Martin oxidation conditions (see Scheme 3).[27] The reaction yields increased with the increase in the number of electron-withdrawing groups introduced in the bodipy core (reactions of **11**, **12,** and **13** were quenched before completion due to formation of side products). The resultant compounds **11**, **12**, **13**, **14**, **15**, and **16** were obtained in 74%, 80%, 80%, 86%, 91%, and 97% yields, respectively.

Electrochemistry of Bodipy Dyes. In order to monitor how electron-withdrawing and -donating groups at positions C2 and

(24) Dilution was necessary to avoid decomposition of the dipyrromethane hydrochloride intermediate, which was otherwise observed upon addition of an excess of DIPEA and $BF_3 \cdot OEt_2$.

(25) (a) Prieto, J. B.; Arbeloa, T.; Liras, M.; Martínez, V. M.; Arbeloa, F. L. *J. Photochem. Photobiol. A: Chem.* **2006**, *184*, 298–305. (b) Cieslik-Boczula, K.; Burgess, K.; Li, L. L.; Nguyen, B.; Pandey, L.; De Borggraeve, W. M.; Van der Auweraer, M.; Boens, N. *Photochem. Photobiol. Sci.* **2009**, *8*, 1006–1015.

(26) Arbeloa, F. L.; Prieto, J. B.; Martínez, V. M.; López, T. A.; Arbeloa, I. L. *ChemPhysChem* **2004**, *5*, 1762–1771.

(27) Meyer, S. D.; Schreiber, S. L. *J. Org. Chem.* **1994**, *59*, 7549–7552.

Scheme 3. Conversion of *meso*-Hydroxymethyl to *meso*-Formyl Bodipy

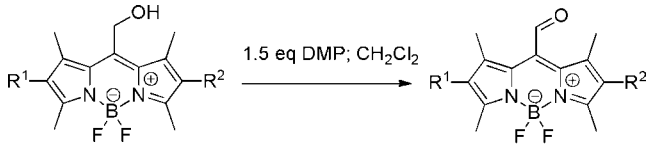

	R^1	R^2	yield
11	Et	Et	74%
12	H	Cl	80%
13	Cl	Cl	80%
14	H	H	86%
15	H	CN	91%
16	CN	CN	97%

C6 modify the redox potential of the bodipy dyes we next conducted electrochemical studies on compounds **1**−**16** and compared these with similar studies we previously performed on PM605 and PMOH.[13]

The redox potentials of the bodipy dyes were measured via cyclic voltammetry. Throughout, acetonitrile solutions and a scan rate of 0.2 V/s and up to 10 V/s were used. All measurements were performed in Ar-saturated solutions 0.1 M in tetrabutylammonium hexafluorophosphate and 0.4 mM in the internal standard ferrocene (Fc/Fc^+). Solutions were ca. 0.72 mM for each of the bodipy dyes studied, as determined from their absorption and extinction coefficients.

The cyclic voltammograms for compounds **1**−**16**, PM605, and PMOH are shown in Figure 2. Table 1 summarizes the electrochemical data. Similar trends were noticed within each group, i.e., for acetoxymethyl, hydroxymethyl, and formyl derivatives. Introduction of H and/or electron-withdrawing groups (e.g., Cl or CN) at positions C2 and C6 leads to an increase in both the reduction and the oxidation potentials with respect to Et-substituted bodipy chromophores.

The acetoxymethyl derivatives appeared to be more versatile in their electrochemistry than either the hydroxymethyl- or the formyl-substituted bodipy dyes. Compounds **1**−**4** showed irreversible reduction and oxidation waves when scanning at 0.2 V/s. Scanning in the negative direction gave two reduction peaks for **1**, **2**, and **4** with E_{pc} values of −1.44 and −1.64 V for **1** and −1.30 and −1.44 V for **2**. For compound **4** the two peaks overlapped into one two-electron peak as can be judged by comparing the integral of the peak with that of the ferrocene standard. Electrochemical reversibility was not observed for these three acetoxymethyl derivatives at scan rates up to 10 V/s. This is in agreement with the electrochemical studies reported for PM605.[13] Compound **3** showed one irreversible reduction peak at a scan rate of 0.2 V/s, which became reversible only at a 10 V/s scan rate. Compound **5** had a different electrochemistry compared to the other acetoxymethyl derivatives. As expected, it showed a much higher reduction potential due to the electron-withdrawing cyano groups at positions C2 and C6. It was the only compound in its group that had reversible reduction at a 0.2 V/s scanning rate ($E°_{B/B^{-\cdot}} = -0.77$ V). A different behavior was observed for oxidation of all acetoxymethyl derivatives compared to PM605. While the oxidation peak for PM605 was reversible at a 0.2 V/s scan rate, all other acetoxymethyl derivatives gave an irreversible oxidation peak at the same scan rate. Their oxidation became reversible only at scan rates of 10 V/s, and the oxidation potential increased in the order from **1** to **5**.

One-electron oxidation and reduction waves were observed for alcohols PMOH and **6**−**10**. A reversible reduction was recorded for PMOH and compounds **6**−**9**, whereas **10** did not show reversibility even at scan rates of 10 V/s. Unlike PMOH, **6**, and **7**, which showed reversible oxidation at 200 mV/s, and **8**, which showed reversible oxidation at 1 V/s, compounds **9** and **10** did not display reversible oxidation at scan rates up to 10 V/s.

The cyclic voltammograms of *meso*-formyl bodipy dyes had two one-electron reduction waves (reversible at scan rates of 0.2 V/s) and a one-electron oxidation wave. We assigned the first reduction wave (at higher potential) to the one-electron reduction of the carbonyl group and the second wave (at lower potential) to the one-electron reduction of the bodipy core. The oxidation wave was reversible at scan rates of 0.2 V/s only for **11** and **12**. Reversibility was observed for **13** and **14** at scan rates of 1 V/s, whereas compounds **15** and **16** remained irreversible even at 10 V/s scan rates. The reduction and oxidation potentials followed the same trend as the acetoxy-

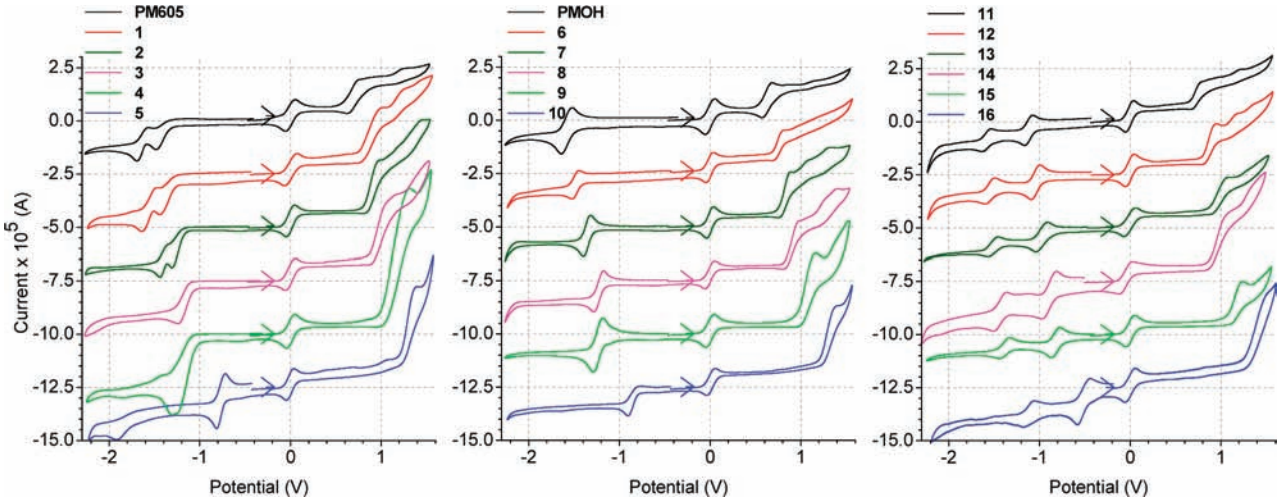

Figure 2. Cyclic voltammograms for 0.72 μM solutions of compounds **1**−**16**, PM605, and PMOH. Note that the plots are offset by 25 μA with respect to each other in the ordinate axis to facilitate comparison. Voltammograms were acquired in degassed, Ar-saturated acetonitrile (0.1 M tetrabutylammonium hexafluorophosphate) versus 0.40 mM Fc/Fc^+. Scan rate = 200 mV s^{-1}. The scan direction is indicated by an arrow. The wave at a potential = 0 V corresponds to Fc/Fc^+. All voltammograms were normalized to the ferrocene anodic peak.

Table 1. Electrochemical Data Acquired at 200 mV/s, and HOMO−LUMO Gaps Determined from Spectroscopy and DFT Calculations[a]

	$E_2°_{B/B^{-\cdot}}$	$E_1°_{B/B^{-\cdot}}$	E_{pc1}	E_{pc2}	$E°_{B^{+\cdot}/B}$	E_{pa1}	E_g (eV)[b]	E_g (eV)[c]	E_{00} (eV)[d]	HOMO (eV)[d]
PM605[e]			−1.48	−1.69	0.70		2.18[f]	2.26	2.79	−5.31
1			−1.44	−1.64		0.88	2.32[f]	2.38	2.86	−5.55
2			−1.30	−1.44		0.97	2.27[f]	2.32	2.82	−5.71
3			−1.24			1.07	2.31[f]	2.25	2.77	−5.86
4			−1.24	−1.31		1.31	2.55[f]	2.42	2.87	−6.05
5		−0.77		−1.91		1.39	2.16[f]	2.38	2.84	−6.49
PMOH[e]		−1.58			0.63		2.21[g]	2.28		
6		−1.48			0.77		2.25[g]	2.41		
7		−1.36			0.82		2.18[g]	2.34		
8		−1.23				0.97	2.14[h]	2.28		
9		−1.24				1.15	2.39[f]	2.45		
10			−0.9			1.39	2.29[f]	2.41		
11	−1.58	−1.12			0.73		1.85[g]	N.A.[i]		
12	−1.60	−1.05			0.86		1.91[g]	N.A.[i]		
13	−1.50	−0.97				1.07	1.97[h]	N.A.[i]		
14	−1.44	−0.89				1.05	1.94[h]	N.A.[i]		
15	−1.38	−0.82				1.23	2.05[f]	N.A.[i]		
16	−1.12	−0.52				1.42	1.94[f]	N.A.[i]		

[a] E_{pc} = cathodic peak potential; E_{pa} = anodic peak potential; $E°_{B/B^{-\cdot}}$ = reversible reduction potential; $E°_{B^{+\cdot}/B}$ = reversible oxidation potential; E_g = HOMO-LUMO gap. [b] Obtained from CV measurements. [c] Obtained from the intercept of the normalized absorption and emission spectra. [d] Obtained from DFT calculations; HOMO values are with respect to vacuum. [e] Data from ref 13. [f] Calculated from ($E_{pa} - E_{pc}$) or ($E_1°_{B/B^{-\cdot}} - E_{pc}$) at 0.2 V/s scan rate. [g] Calculated from ($E°_{B^{+\cdot}/B} - E_1°_{B/B^{-\cdot}}$) at 0.2 V/s scan rate. [h] Calculated from ($E°_{B^{+\cdot}/B} - E_1°_{B/B^{-\cdot}}$) at 1 V/s scan rate. [i] Nonavailable due to the lack of emission from *meso*-formyl bodipys.

methyl and hydroxymethyl derivatives and increased with introduction of electron-withdrawing groups.

The observed peak separation for the reversible waves was ca. 100 mV, which is larger than expected for Nernstian behavior, where one-electron waves are expected to have a peak separation of 59 mV. The peak separation for the ferrocence internal standard, which is known to have a Nernstian behavior, was also 100 mV under our experimental conditions (similar results have been previously observed and were attributed to ohmic drop (1 kohm), which is often observed within aprotic solvents).[28] Also, for the reversible reductions and reversible oxidations, the peak current ratios (i_{pa}/i_{pc} or i_{pc}/i_{pa}) were approximately unity, indicating that the radical ions were fairly stable and no additional chemical reactions took place.[29]

We additionally conducted DFT calculations at the B3LYP/6-31G(d) level[30] to estimate the HOMO and LUMO energy levels for compounds **1**−**5**. Table 1 lists the calculated HOMO and LUMO values relative to vacuum as well as the energy band gap for compounds **1**−**5** and PM605.[13] There is a good correlation between electrochemical studies and DFT calculations on the decrease in HOMO and LUMO values with substitution (Et, H, Cl, and CN); there is also a linear dependence on the energy band gaps obtained from spectroscopic studies and those determined from DFT. However, the calculated energy band gap values amply surpass those obtained experimentally (Tables 1 and 2). Ab initio methods have been shown to overestimate the energy gap, but they successfully predict the effect of substitution on spectroscopy based on the electronic densities of HOMO and LUMO orbitals (see below).[7]

Spectroscopy of Bodipy Dyes. Listed in Table 2 are the main photophysical properties of compounds **1**−**16** determined in acetonitrile. Figure 3 displays the absorption and emission spectra for these compounds.

Table 2. Photophysical Properties of Dyes **1**−**16** in Various Solvents at Room Temperature

	abs λ_{max} (nm)	em λ_{max} (nm)	ϕ_f	τ_{dec} (ns)	$\varepsilon \times 10^3$ (M^{-1} cm^{-1})
PM605[b]	542	561	0.72	6.76	70
1	515	530	0.87	6.66	81
2	526	546	0.88	6.31	66
3	543	560	0.68	6.46	58
4	503	526	0.86	4.68	46
5	515	531	0.76	5.24	96
PMOH[b]	536	552	0.84	6.90	70
6	510	523	0.98	6.65	100
7	521	535	0.82	6.31	70
8	537	554	0.79	6.46	53
9	498	517	0.87	4.65	51
10	509	525	1.00	5.05	94
11	535	N.A.	N.A.	N.A.	16
12	509	N.A.	N.A.	N.A.	18
13	520	N.A.	N.A.	N.A.	43
14	538	N.A.	N.A.	N.A.	16
15	499	N.A.	N.A.	N.A.	57
16	510	N.A.	N.A.	N.A.	42

[a] Also shown for comparison are the photophysical properties of the commercially available dye PM605 and its alcohol derivative PMOH. [b] Data from ref 13.

The lowest energy absorption band (S_0 to S_1 0−0 transition) is centered in the green region of the visible spectrum (in the range of 489−566 nm) for compounds **1**−**10**. It shows a higher energy vibronic shoulder at ca. 1100 cm^{-1} from the main peak (in the range of 470−510 nm). For a given family of compounds the absorption and emission bands shift to lower energies when positions C2 and C6 bear electron-donating groups (see Table 2 and Figure 3). A drop of ca. 0.1 eV in the HOMO−LUMO energy gap (E_g) is also observed (see Table 1). Our results are consistent with expectations from previous DFT calculations[7,26] on the electronic density of the HOMO and LUMO for the commercially available bodipy dyes PM567 and PM650 (dyes bearing H or CN groups, respectively, at positions C2 and C6 and a methyl substituent at position C8). These calculations show a significant depletion in the electronic density at positions C2 and C6 in the excited state in comparison to the ground state; it is therefore expected that electron-withdrawing groups such as the nitriles found in compounds **4** and **5** as well as **9**

(28) Lai, R. Y.; Fabrizio, E. F.; Lu, L.; Jenekhe, S. A.; Bard, A. J. *J. Am. Chem. Soc.* **2001**, *123*, 9112–9118.
(29) Lai, R. Y.; Bard, A. J. *J. Phys. Chem. B* **2003**, *107*, 5036–5042.
(30) (a) Frisch, M. J. *Gaussian 03*, Revision C.02; Gaussian, Inc.: Wallingford, CT, 2004. (b) Koch, W.; Holthausen, M. C. *A Chemist's Guide to Density Functional Theory*, 2nd ed.; Wiley-VCH: Weinheim, Germany, 2000.

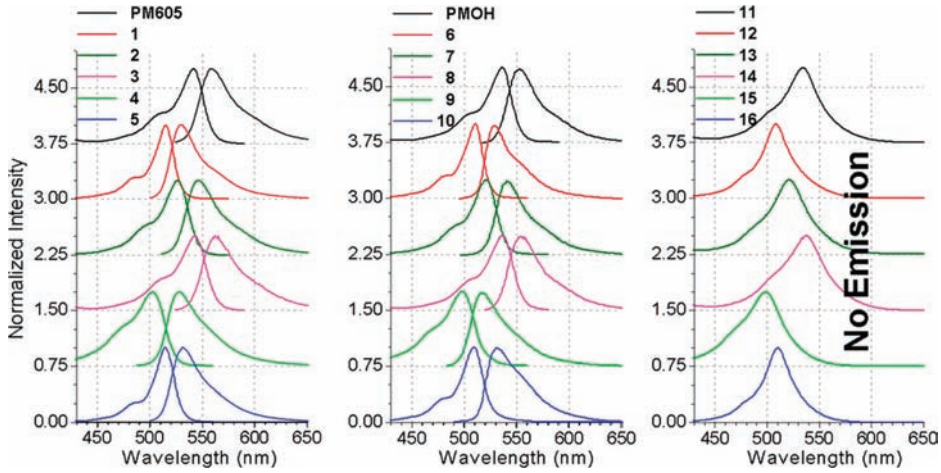

Figure 3. Normalized absorption and emission spectra obtained in acetonitrile for compounds **1**−**16**, PM605, and PMOH. Note that the plots are offset with respect to each other in the ordinate axis to facilitate comparison.

and **10** will increase the HOMO−LUMO energy gap by stabilizing the HOMO relative to the LUMO. On the contrary, electron-donating groups such as ethyl groups in PM605 and PMOH will stabilize the LUMO relative to the HOMO level, thus decreasing the energy gap. Interestingly, in the case of substitution with Cl at C2 and C6 (see compounds **3** and **8**) the resonance (donating) effects dominate over inductive. Thus, the energy gap and absorption and emission λ_{max} for these compounds are comparable to those observed with the bodipy dyes PM605 and PMOH. Asymmetric dyes **2** and **7** (Cl, H) or **4** and **9** (CN, H) all show significantly higher HOMO−LUMO energy gaps than their symmetric counterparts **3** and **8** (Cl, Cl) or **5** and **10** (CN, CN).

The lower absorption, emission, and band gap energies measured for the acetoxymethyl-substituted bodipy dyes compared to their hydroxymethyl-substituted counterparts may be rationalized by the electron-withdrawing nature of the acyl group (compare PM605 and compounds **1**−**5** vs PMOH and compounds **6**−**10**, respectively). Since ab initio calculations have shown an increase in electron density in the meso position for the LUMO vs the HOMO level, the acyl groups will preferentially stabilize the former over the latter.[7,26]

The fluorescence lifetimes for *meso*-acetoxymethyl (PM605 and **1**−**3**) or *meso*-hydroxymethyl (PMOH and **6**−**8**) bodipy dyes range between 6.5 and 7.5 ns with the exception of the nitrile-bearing bodipy dyes **4**, **5**, **9**, and **10**. The fluorescence lifetimes for the latter compounds are somewhat shorter; we recorded values in the range of 4.65−5.24 ns in all solvents. Given the high emission quantum yields for **4**, **5**, **9**, and **10** (see Table 2), the shorter lifetimes indicate a faster radiative decay taking place in 2- or 2,6-CN-substituted bodipy chromophores. We were not able to measure fluorescence lifetimes for compounds **11**−**16** since they are nonemissive (see below).

The absorption spectra of *meso*-formyl bodipy dyes **11**−**16** are unique since they display an additional (lower energy) transition buried within the major absorption peak, extending beyond 600 nm for some of these compounds, which is likely arising from a $n-\pi^*$ transition. These absorption spectra are much broader than the ones recorded for compounds **1**−**10** (Figure 3). *meso*-Formyl bodipy dyes also have a smaller HOMO−LUMO energy gap when compared to their hydroxymethyl and acetoxymethyl counterparts, as observed from the electrochemical studies (Table 1); this is consistent with a lower energy $n-\pi^*$ transition. No reliable HOMO−LUMO energy gap estimation can be done for **11**−**16** based on spectroscopic measurements due to their lack of emission (see below).

Scheme 4. Hemiacetal Formation in Methanol

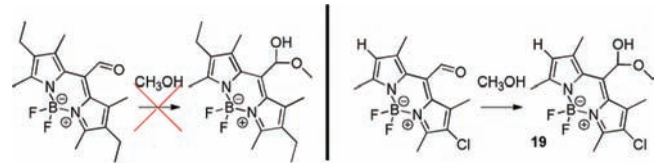

The most striking difference between compounds **1**−**10**, PMOH, and PM605 vs compounds **11**−**16** is the difference in emission quantum yield (ϕ_f) and molar extinction coefficient (ε), reflecting the forbidden nature of the lowest energy electronic excitation and emission transition for the *meso*-formyl bodipy dyes. Compounds **1**−**10** together with PM605 and PMOH have high molar extinction coefficients (70 000−90 000 M^{-1} cm^{-1}) and relatively high fluorescence quantum yield values ranging from 0.7 to 1 in acetonitrile. Substituents at positions C2 and C6 do not dramatically affect either the ϕ_f or the molar extinction coefficient. In marked contrast, *meso*-formyl bodipy dyes show up to 4-fold reduction in the molar extinction coefficient (16 000−60 000 M^{-1} cm^{-1}). Most importantly, these compounds are nonemissive. No emission was recorded upon exciting these compounds at their absorption maximum.

The nonemissive formyl dyes provide unique opportunities as fluorogenic probes of nucleophilic attack by, e.g., alcohols and amine groups. Studies conducted in our group reveal that emission is rapidly restored following hemiacetal formation upon addition of **13** to methanol at room temperature (compound **19**, Scheme 4 and Figure 4). Compound **11**, being much less reactive toward nucleophiles, did not react with methanol under the same conditions, and no emission enhancement was observed. Compound **13** readily underwent reaction with *n*-butyl amine to form nonemissive intermediate imine **21**, which upon reduction gave a highly emissive **23** with ϕ_f values of 0.9 in toluene. A catalyst and high temperatures (90 °C in toluene) were however required to form the corresponding imine **20** following reaction of **11** and *n*-butyl amine.[31] Reduction of **20** in methanol yielded **22** with ϕ_f values of 0.13 in acetonitrile. *meso*-Formyl bodipy dyes

(31) Hall, H. K., Jr.; Padias, A. B.; Williams, P. A.; Gosau, J.-M.; Boone, H. W.; Park, D.-K. *Macromolecules* **1995**, *28*, 1–8.

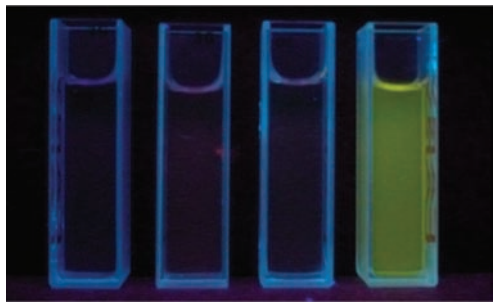

Figure 4. From left to right, solutions of compounds **11** in acetonitrile and methanol and solutions of compound **13** in acetonitrile and methanol, all at room temperature, portrayed upon UV excitation. Rapid emission enhancement was observed upon preparing the solution in methanol due to nucleophilic addition of methanol to compound **13**.

with electron-withdrawing groups at positions C2 and C6 are highly reactive given their enhanced electrophilicty.

Conclusion

New bodipy dyes were obtained with versatile tethering potential and diverse electrochemical properties. Hydroxymethyl or formyl groups at the meso position provided a handle for covalent tethering to receptors and biomolecules of interest, which dispenses with the more commonly used *meso*-aryl moiety as a means to tag molecules and thus avoid the undesired internal conversion dissipation mechanisms attributed to such a moiety. The new dyes may be coupled to both electrophiles and nucleophiles. Substitution at positions C2 and C6 with electron-withdrawing or -donating groups (Et, H, Cl or CN) enabled tuning the redox protentials within a ca. 0.7 eV; importantly, no substantial changes were observed in either the absorption or the emission spectra or the HOMO−LUMO band gap. *meso*-Acetoxymethyl and *meso*-hydroxymethyl bodipy dyes showed, in general, irreversible and reversible electrochemical reductions, respectively. In the case of *meso*-formyl compounds a reversible two-electron reduction was recorded. A one-electron electrochemical oxidation was recorded for all compounds reported. *meso*-Acetoxymethyl and *meso*-hydroxymethyl are characterized by their high emission quantum yields (in the range of 0.7−1) and extinction coefficients (in the range of 50 000−100 000). Fluorescence lifetimes in the range of 4.5−7.0 ns are further recorded for these compounds. In contrast, *meso*-formyl compounds show an up to 4-fold reduction in the molar extinction coefficient and are nonemissive, consistent with a forbidden $n-\pi^*$ transition from the ground state to the lowest singlet excited state. The nonemissive *meso*-formyl bodipy dyes thus provide unique opportunities as fluorogenic probes of nucleophilic attack by, e.g., alcohols, thiols, and amine groups and as fluorescent labeling agents where uncoupled fluorophores will not contribute to the fluorescence background. Overall, the new bodipy dyes reported here are promising candidates for the preparation of fluorescent sensors relying in photoinduced electron transfer and may find use in a number of fluorescent-labeling protocols.

Experimental Section

Materials. 8-Acetoxymethyl-2,6-diethyl-1,3,5,7-tetramethylpyrromethene fluoroborate (PM605) was purchased from Exciton, Inc. All other chemicals were supplied by Sigma-Aldrich, Co. and used without further purification.

Instrumentation. Absorption and emission spectra were recorded on a Cary 5000 UV−vis−NIR and Cary Eclipse Fluorescence Spectrophotomeres using 1 cm ×1 cm quartz quvettes. ^{1}H NMR and ^{13}C NMR spectra were recorded on a Varian VNMRS 500 instrument at 500 and 125 MHz, respectively. ESI mass spectra were measured on a Thermo Scientific Exactive Orbitrap. Voltammetric experiments were conducted with a computer-controlled CHI760C potentiostat with a BASi C3 cell stand.

Fluorescence Quantum Yield. PM605 in ethanol ($\phi_{st} = 0.74$) was used as a standard to calculate the emission quantum yields of the compounds (ϕ_x). The absorption spectra of solutions of PM605 in ethanol and the dye of interest in acetonitrile at five different concentrations were matched at 375 nm. Emission spectra were recorded for all solutions using excitation and emission slits of 2.5 nm upon excitation at 375 nm. Relative quantum efficiencies with respect to the standard were obtained from the slope of the product of absorption for the standard A_{st}, integrated emission I_x, and solvent refractive index n_x for the unknown ϕ_x vs the product of absorption for the unknown A_x, integrated emission I_{st}, and solvent refractive index n_{st} for the standard (see eq 1 below).

$$A_{st}I_x n_x^2 = \frac{\phi_x}{\phi_{st}} A_x I_{st} n_{st}^2 \quad (1)$$

Electrochemical Studies. Electrochemical experiments were performed using a three-electrode system. The working electrode was 2 mm Pt with a Pt wire as auxilary electrode and a 0.01 M $Ag/AgNO_3$ solution reference electrode. A 0.1 M solution of tetrabutylammonium hexafluorophosphate in dry acetonitrile was used as the electrolyte solvent in which the compounds were dissolved to a final 0.72 mM concentration. Solutions also contained ferrocene with a concentration of 0.40 mM as an internal standard. The solutions were purged with argon, and all measurements were conducted under inert atmosphere. Formal redox potentials were calculated from the midpoint of the cathodic and anodic peak potentials observed in the cyclic voltammograms. All values were reported vs ferrocene, with the oxidation of ferrocene measured and corrected to zero for all experiments.

Fluorescence Lifetime Studies. The fluorescence lifetime measurements were carried out using a Picoquant Fluotime 200 Time Correlated Single Photon Counting setup employing an LDH 470 ps diode laser (Picoquant) with an excitation wavelength at 466 nm as the excitation source. The laser was controlled by a PDL 800 B picosecond laser driver from Picoquant. The excitation rate was 10 MHz, and the detection frequency was less than 100 kHz. Photons were collected at the magic angle.

8-Hydroxymethyl-2,6-diethyl-1,3,5,7-tetramethyl Pyrromethene Fluoroborate, PMOH. 8-Hydroxymethyl-2,6-diethyl-1,3,5,7-tetramethyl pyrromethene fluoroborate was prepared as described in the literature.[21]

3-Cyano-2,4-dimethyl Pyrrole, 17. 17 was prepared as described in the literature with minor modifications.[17,23] A mixture of 3-aminocrotonitrile (1.46 g, 17.8 mmol, 2 equiv) and glycine *N*′-methoxy-*N*′-methylamide HBr salt (1.77 g, 8.89 mmol, 1 equiv) in dry ethanol was stirred under argon at 50 °C. After 16 h the reaction mixture was concentrated in vacuo. The solid residue was washed with DCM, and the organic fractions were concentrated. The solid residue was used for the next step without further purification. The overall yield of 3-cyano-2,4-dimethyl pyrrole was 54%: ^{1}H NMR (500 MHz, $CDCl_3$) δ 8.38 (br, 1H), 6.38 (s, 1H), 2.37 (s, 3H), 2.13 (s, 3H); ^{13}C NMR (125 MHz, $CDCl_3$) δ 136.9, 121.8, 117.1, 114.7, 92.6, 12.3, 10.6.

8-Acetoxymethyl-1,3,5,7-tetramethyl Pyrromethene Fluoroborate, 1. 2,4-Dimethyl pyrrole (0.2 g, 2.1 mmol, 2 equiv) was dissolved in dry CH_2Cl_2. Acetoxyacetyl chloride (0.14 mL, 1.3 mmol, 1.2 equiv) was added to the solution, and the reaction was left stirring at 40 °C under argon. After 2 h, it was cooled to room temperature and diisopropylethylamine (0.73 mL, 4.2 mmol, 4 equiv) was added followed after 15 min by dropwise addition of $BF_3 \cdot OEt_2$ (0.53 mL, 4.2 mmol, 4 equiv). During addition of $BF_3 \cdot OEt_2$ the color changed from pale yellow to dark red. The

reaction was stopped after 15 min, the solvent was evaporated under reduced pressure, and the crude reaction mixture was loaded onto a silica gel flash column and eluted with 50% ethyl acetate/hexane to give **1** as orange-green crystals (0.25 g, 75% yield): ^{1}H NMR (500 MHz, $CDCl_3$) δ 6.08 (s, 2H), 5.29 (s, 2H), 2.53 (s, 6H), 2.35 (s, 6H), 2.13 (s, 3H); ^{13}C NMR (125 MHz, $CDCl_3$) δ 170.5, 156.6, 141.5, 133.3, 132.6, 122.3, 57.8, 20.6, 15.6, 14.7; HRMS (ESI) for $C_{16}H_{19}N_2O_2BF_2$ (M + Na) calcd 343.1400, found 343.1396; FTIR 965, 1074, 1190, 1510, 1551, 1742 cm^{-1}.

8-Acetoxymethyl-2-chloro-1,3,5,7-tetramethyl Pyrromethene Fluoroborate, 2. 8-Acetoxymethyl-1,3,5,7-tetramethyl pyrromethene fluoroborate, **1** (0.2 g, 0.62 mmol, 1 equiv), was dissolved in 3 mL of dry THF under argon and cooled to −78 °C. *N*-Chlorosuccinimide (0.17 g, 1.3 mmol, 2 equiv) dissolved in 2 mL of dry THF was added dropwise to the solution. The reaction mixture was stirred for 15 min at −78 °C, after which it was warmed to room temperature and stirred for an additional 12 h. The solution was diluted with CH_2Cl_2 and washed with brine. The organic layer was dried with $MgSO_4$, and the solvent was next evaporated under reduced pressure. The solid residue was loaded onto a silica gel flash column and eluted with dichloromethane to give **2** as red-green crystals (0.17 g, 76% yield): ^{1}H NMR (500 MHz, $CDCl_3$) δ 6.13 (s, 1H), 5.28 (s, 2H), 2.54 (s, 6H), 2.37 (s, 3H), 2.33 (s, 3H), 2.13 (s, 3H); ^{13}C NMR (125 MHz, $CDCl_3$) δ 170.4, 159.2, 151.1, 143.3, 134.5, 133.7, 133.5, 130.1, 123.2, 123.1, 122.4, 57.8, 20.5, 15.8, 14.8, 12.7, 12.4; HRMS (ESI) for $C_{16}H_{18}N_2O_2BClF_2$ (M + Na) calcd 377.10101, found 377.10206; FTIR 643, 720, 965, 1160,1183, 1552, 1742 cm^{-1}.

8-Acetoxymethyl-2,6-dichloro-1,3,5,7-tetramethyl Pyrromethene Fluoroborate, 3. 8-Acetoxymethyl-1,3,5,7-tetramethyl pyrromethene fluoroborate, **1** (0.2 g, 0.62 mmol, 1 equiv), was dissolved in 3 mL of dry THF under argon and cooled to −78 °C. *N*-Chlorosuccinimide (0.33 g, 2.5 mmol, 4 equiv) dissolved in 2 mL of dry THF was added dropwise to the solution. The reaction mixture was stirred for 15 min at −78 °C, after which it was warmed to room temperature and stirred for an additional 36 h. The solution was diluted with CH_2Cl_2 and washed with brine. The organic layer was dried with $MgSO_4$, and the solvent was evaporated under reduced pressure. The solid residue was loaded onto a silica gel flash column and eluted with dichloromethane to give **3** as purple-green crystals (0.22 g, 92% yield). ^{1}H NMR (500 MHz, $CDCl_3$) δ 5.29 (s, 2H), 2.57 (s, 6H), 2.36 (s, 6H), 2.14 (s, 3H); ^{13}C NMR (125 MHz, $CDCl_3$) δ 170.3, 153.7, 136.2, 134.1, 130.9, 123.6, 57.7, 20.6, 12.9, 12.6; HRMS (ESI) for $C_{16}H_{17}N_2O_2BCl_2F_2$ (M^-) calcd 387.06554, found 387.06563; FTIR 600, 720, 992, 1178, 1555, 1742 cm^{-1}.

8-Acetoxymethyl-2-cyano-1,3,5,7-tetramethyl Pyrromethene Fluoroborate, 4. 3-Cyano-2,4-dimethyl-pyrrole, **17** (0.2 g, 1.7 mmol, 1 equiv) was dissolved in acetoxyacetyl chloride (0.91 mL, 8.5 mmol, 5 equiv). The reaction was left stirring at 45 °C under argon for 4 h until it turned dark green. The solution was evaporated to dryness under reduced pressure and dried under vacuum for 1 h. A green solid (**18**) was obtained, which was redissolved in 2 mL of dry dichlomethane to yield a ca. 1 M solution of **18** to which 2,4-dimethylpyrrole (0.21 mL, 2.1 mmol, 1.2 equiv) was added. The solution was refluxed at 40 °C under argon for 1 h. The reaction mixture was next cooled to room temperature, and 8 mL of dry dichloromethane was added (0.1 M solution). After addition of diisopropylethylamine (1.2 mL, 6.8 mmol, 4 equiv) the solution turned pale yellow. The reaction was left stirring for 15 min. $BF_3\cdot OEt_2$ (1.5 mL, 13.6 mmol, 8 equiv) was next added dropwise. The color changed from pale yellow to dark red after a few minutes. After 30 min the reaction was stopped. The solvent was evaporated under reduced pressure, and the residue was loaded onto a silica gel flash column and eluted with dichloromethane to give **4** as an orange powder (0.13 g, 46% yield): ^{1}H NMR (500 MHz, $CDCl_3$) δ 6.28 (s, 1H), 5.32 (s, 2H), 2.63 (s, 3H), 2.60 (s, 3H), 2.48 (s, 3H), 2.45 (s, 3H), 2.14 (s, 3H); ^{13}C NMR (125 MHz, $CDCl_3$) δ 170.2, 164.7, 154.7, 146.6, 140.4, 136.2, 134.9, 129.8, 125.7, 114.8, 57.3, 20.5, 16.3, 15.4, 14.0, 13.4; HRMS (ESI) for $C_{17}H_{18}N_3O_2BF_2$ (M + Na) calcd 368.1352, found 368.1347; FTIR 1033, 1109, 1224, 1579, 1738, 2215 cm^{-1}.

8-Acetoxymethyl-2,6-dicyano-1,3,5,7-tetramethyl Pyrromethene Fluoroborate, 5. 3-Cyano-2,4-dimethyl-pyrrole, **17** (0.8 g, 6.7 mmol, 2 equiv), was dissolved in dry CH_2Cl_2 to yield a 3 M solution. Acetoxyacetyl chloride (0.43 mL, 4 mmol, 1.2 equiv) was added to the solution, and the reaction was left stirring at 40 °C under argon for 24 h until it turned dark green. The reaction mixture was allowed to cool to room temperature, and the solution was diluted to 0.3 M with dry CH_2Cl_2. Diisopropylethylamine (2.3 mL, 13.4 mmol, 4 equiv) was added, after which the reaction mixture turned pale yellow. The reaction was left stirring at room temperature under argon for 15 min. $BF_3\cdot OEt_2$ (1.7 mL, 13.4 mmol, 4 equiv) was added dropwise. The color changed from pale yellow to dark red after a few minutes. The reaction was stopped after 15 min. The solvent was evaporated under reduced pressure, and the crude reaction mixture was loaded onto a silica gel flash column and eluted with 50% ethyl acetate/hexane followed by a second silica gel flash column with CH_2Cl_2 to give **5** as a red powder (0.76 g, 31% yield): ^{1}H NMR (500 MHz, $CDCl_3$) δ 5.36 (s, 2H), 2.71 (s, 6H), 2.61 (s, 6H), 2.16 (s, 3H); ^{13}C NMR (125 MHz, $CDCl_3$) δ 170.1, 160.9, 148.1, 139.4, 132.9, 113.5, 57.1, 20.7, 15.4, 14. 3; HRMS (ESI) for $C_{18}H_{17}N_4O_2BF_2$ (M^-) calcd 369.1329, found 369.1329; FTIR 1004, 1189, 1551, 1736, 2222 cm^{-1}.

General Procedures for the Hydrolysis of Acetoxy Bodipy Derivatives. Procedure 1. *meso*-Acetoxymethyl bodipy dyes **1**, **3**, and **5** (1 equiv) were dissolved in dry THF under argon to yield a 0.05 M solution. $LiOH\cdot H_2O$ (5 equiv) was dissolved in a volume of water equal to the volume of THF employed in dissolving the bodipy dye. The aqueous LiOH solution and the bodipy solution in THF were combined. The reaction mixture was left stirring for 4 h at room temperature under argon and then extracted with ethyl acetate (3 × 100 mL). The combined organic layers were washed with saturated aqueous NH_4Cl solution (3 × 100 mL) and brine (1 × 100 mL) and dried over $MgSO_4$, filtered, and evaporated under reduced pressure to afford the corresponding alcohol as an amorphous solid. The crude product was loaded onto a silica gel flash column and eluted with 50% ethyl acetate/hexane.

Procedure 2. *meso*-Acetoxymethyl bodipy dyes **2** and **4** (1 equiv) were dissolved in acetone to yield 0.02 M solution. A 4 M HCl solution in water was added to the solution for a final HCl concentration of 1.3 M. The reaction mixture was stirred at 40 °C under argon until the starting material was consumed. The solution was diluted with ethyl acetate, washed with brine three times, and dried over $MgSO_4$, and the solvent was evaporated under reduced pressure. The crude product was purified by flash column chromatography with 50% ethyl acetate/hexane.

8-Hydroxymethyl-1,3,5,7-tetramethyl Pyrromethene Fluoroborate, 6. 8-Acetoxymethyl-1,3,5,7-tetramethyl pyrromethene fluoroborate, 1 (0.2 g, 0.62 mmol), was stirred for 4 h in the presence of LiOH (0.13 g, 3.1 mmol) according to procedure 1 described above to give **6** as an orange powder (0.12 g, 70%). ^{1}H NMR (500 MHz, d_6-DMSO) δ 6.21 (s, 2H), 5.52 (t, 1H), 4.70 (d, J = 5.1 Hz, 2H), 2.47 (s, 6H), 2.39 (s, 6H); ^{13}C NMR (125 MHz, d_6-DMSO) δ 154.9, 142.5, 141.4, 132.2, 122.0, 54.6, 15.6, 14.7; HRMS (ESI) for $C_{14}H_{17}N_2OBF_2$ (M + Na) calcd 301.1294, found 301.1292; FTIR 958, 1156, 1203, 1510, 1558, 3549 cm^{-1}.

8-Hydroxymethyl-2-chloro-1,3,5,7-tetramethyl Pyrromethene Fluoroborate, 7. 8-Acetoxymethyl-2-chloro-1,3,5,7-tetramethyl pyrromethene fluoroborate, **2** (0.15 g, 0.42 mmol, 1 equiv), was stirred for 16 h in the presence of HCl according to procedure 2 described above to give **7** as a red powder with quantitative yield (0.13 g). ^{1}H NMR (500 MHz, d_6-DMSO) δ 6.35 (s, 1H), 5.62−5.64 (t, 1H), 4.70−4.71 (d, J = 5.1 Hz, 2H), 2.50 (s, 3H), 2.45 (s, 3H), 2.44 (s, 3H), 2.41 (s, 3H); ^{13}C NMR (125 MHz, d_6-DMSO) δ 158.9, 147.7, 145.5, 141.9, 134.8, 133.4, 129.5, 123.6, 120.4, 54.6, 15.9, 14.9, 12.6, 12.4; HRMS (ESI) for $C_{14}H_{16}N_2OBClF_2$ (M^-) calcd 311.09395, found 311.09379; FTIR 648, 720, 978, 1308, 1552, 3544 cm^{-1}.

8-Hydroxymethyl-2,6-dichloro-1,3,5,7-tetramethyl Pyrromethene Fluoroborate, 8. 8-Acetoxymethyl-2,6-dichloro-1,3,5,7-tetramethyl pyrromethene fluoroborate, **3** (0.22 g, 0.57 mmol), was stirred for 4 h in the presence of LiOH (0.12 g, 2.9 mmol) according to procedure 1 described above to give **8** as red-green crystals (0.17 g, 84%). ^{1}H NMR (500 MHz, $CDCl_3$) δ 4.92−4.91 (d, J = 5.1 Hz, 2H), 2.55 (s, 6H), 2.50 (s, 6H); ^{13}C NMR (125 MHz, $CDCl_3$) δ 153.3, 138.6, 136.1, 130.5, 123.3, 55.9, 22.9, 12.9, 12.6; HRMS (ESI) for $C_{14}H_{15}N_2OBCl_2F_2$ (M^-) calcd 345.05498, found 345.05507; FTIR 606, 718, 996, 1052, 1552, 3544 cm^{-1}.

8-Hydroxymethyl-2-cyano-1,3,5,7-tetramethyl Pyrromethene Fluoroborate, 9. 8-Acetoxymethyl-2-cyano-1,3,5,7-tetramethyl pyrromethene fluoroborate, **4** (0.08 g, 0.23 mmol, 1 equiv), was stirred for 4 h in the presence of HCl according to procedure 2 described above to give **9** as an orange powder with quantitative yield. ^{1}H NMR (500 MHz, $CDCl_3$) δ 6.27 (s, 1H), 4.93 (s, 2H), 2.63 (s, 3H), 2.62 (s, 3H), 2.59 (s, 3H), 2.56 (s, 3H); ^{13}C NMR (125 MHz, $CDCl_3$) δ 164.0, 154.5, 146.5, 140.4, 139.3, 135.6, 129.5, 125.4, 114.9, 55.7, 16.2, 15.3, 13.9, 13.4; HRMS (ESI) for $C_{15}H_{16}N_3OBF_2$ (M^-) calcd 302.12817, found 302.12786; FTIR 976, 1063, 1190, 1558, 2223, 3537 cm^{-1}.

8-Hydroxymethyl-2,6-dicyano-1,3,5,7-tetramethyl Pyrromethene Fluoroborate, 10. 8-Acetoxymethyl-2,6-dicyano-1,3,5,7-tetramethyl pyrromethene fluoroborate, **5** (0.2 g, 0.54 mmol), was stirred for 4 h in the presence of LiOH (0.11 g, 2.7 mmol) according to procedure 1 described above to give **10** as a red powder (0.15 g, 83%). ^{1}H NMR (400 MHz, d_6-acetone) δ 2.85 (s, 2H), 2.78 (s, 6H), 2.66 (s, 6H); ^{13}C NMR (75 MHz, d_6-acetone) δ 158.9, 148.5, 146.7, 132.5, 113.1, 54.8, 14.1, 13.0; HRMS (ESI) for $C_{16}H_{15}N_4OBF_2$ (M^-) calcd 327.1223, found 327.1227; FTIR 1000, 1197, 1551, 2223, 3549 cm^{-1}.

General Procedure for the Synthesis of Aldehyde Bodipy Derivatives (Dess−Martin Oxidation). Dess−Martin periodinane (1.5 equiv) was dissolved in dry dichloromethane. To the suspension was slowly added a solution of *meso*-acetoxymethyl bodipy dyes PMOH, **6**, **7**, **8**, **9**, and **10** (1 equiv) in dry dichloromethane at 0 °C under argon. After 10 min, the ice bath was removed and the reaction mixture was left stirring at room temperature for extended periods of time as detailed below. The reaction mixture was extracted with saturated aqueous $Na_2S_2O_3$ followed by saturated aqueous $NaHCO_3$ and brine. The combined organic solutions were dried over $MgSO_4$. The solvent was evaporated, and the residue was purified using flash column chromatography with dichloromethane as the eluent.

8-Formyl-2,6-diethyl-1,3,5,7-tetramethyl Pyrromethene Fluoroborate, 11. Reaction of 8-hydroxymethyl-2,6-diethyl-1,3,5,7-tetramethyl pyrromethene fluoroborate, PMOH (0.1 g, 0.3 mmol), and Dess−Martin periodinane (0.19 g, 0.45 mmol) took place for 15 min according to the procedure described above to give **11** as a purple powder (0.073 g, 74%). ^{1}H NMR (500 MHz, $CDCl_3$) δ 10.61 (s, 1H), 2.51 (s, 6H), 2.39−2.34 (q, J = 7.6 Hz, J = 7.5 Hz, 4H), 2.04 (s, 6H), 1.05−1.02 (t, J = 7.7 Hz, J = 7.5 Hz, 6H); ^{13}C NMR (125 MHz, $CDCl_3$) δ 194.1, 156.7, 136.4, 134.8, 133.6, 17.1, 14.6, 12.9, 12.8; HRMS (ESI) for $C_{18}H_{23}N_2OBF_2$ (M^-) calcd 333.19443, found 333.19453; FTIR:, 979, 1183, 1319, 1551, 1711 cm^{-1}.

8-Formyl-1,3,5,7-tetramethyl Pyrromethene Fluoroborate, 12. Reaction of 8-hydroxymethyl-1,3,5,7-tetramethyl pyrromethene fluoroborate, **6** (0.1 g, 0.35 mmol), and Dess−Martin periodinane (0.23 g, 0.53 mmol) took place for 30 min according to the procedure described above to give **12** as a brown-green powder (0.083 g, 86%). ^{1}H NMR (500 MHz, $CDCl_3$) δ 10.57 (s, 1H), 6.08 (s, 2H), 2.54 (s, 6H), 2.13 (s, 6H); ^{13}C NMR (125 MHz, $CDCl_3$) δ 193.0, 158.5, 141.5, 135.9, 128.8, 121.8, 30.9, 15.4, 14.8; HRMS (ESI) for $C_{14}H_{15}N_2OBF_2$ (M^-) calcd 275.11727, found 275.11677; FTIR 965, 1061, 1190, 1306, 1510, 1558, 1715 cm^{-1}.

8-Formyl-2-chloro-1,3,5,7-tetramethyl Pyrromethene Fluoroborate, 13. Reaction of 8-hydroxymethyl-2-chloro-1,3,5,7-tetramethyl pyrromethene fluoroborate, **7** (0.1 g, 0.32 mmol), and Dess−Martin periodinane (0.2 g, 0.48 mmol) took place for 15 min according to the procedure described above to give **13** as a purple-green powder (0.08 g, 80%). ^{1}H NMR (500 MHz, $CDCl_3$) δ 10.54 (s, 1H), 6.11, (s, 1H), 2.54, (s, 6H), 2.12 (s, 3H), 2.09 (s, 3H); ^{13}C NMR (125 MHz, $CDCl_3$) δ 192.6, 160.9, 152.8, 143.2, 136.1, 134.7, 129.6, 126.0, 122.6, 122.3, 15.5, 15.0, 12.7, 12.5; HRMS (ESI) for $C_{14}H_{14}N_2OBClF_2$ (M^-) calcd 309.07830, found 309.07788; FTIR 642, 818, 1550, 1710 cm^{-1}.

8-Formyl-2,6-dichloro-1,3,5,7-tetramethyl Pyrromethene Fluoroborate, 14. Reaction of 8-hydroxymethyl-2,6-dichloro-1,3,5,7-tetramethyl pyrromethene fluoroborate, **8** (0.1 g, 0.29 mmol), and Dess−Martin periodinane (0.18 g, 0.43 mmol) took place for 30 min according to the procedure described above to give **14** as a purple-green powder (0.08 g, 80%). ^{1}H NMR (500 MHz, $CDCl_3$) δ 10.55 (s, 1H), 2.57 (s, 6H), 2.12 (s, 6H); ^{13}C NMR (125 MHz, $CDCl_3$) δ 192.1, 155.5, 136.3, 136.2, 126.9, 123.4, 12.9, 12.8; HRMS (ESI) for $C_{14}H_{13}N_2OBCl_2F_2$ (M^-) calcd 343.03933, found 343.03892; FTIR 600, 676, 990, 1182, 1554, 1716 cm^{-1}.

8-Formyl-2-cyano-1,3,5,7-tetramethyl Pyrromethene Fluoroborate, 15. Reaction of 8-hydroxymethyl-2-cyano-1,3,5,7-tetramethyl pyrromethene fluoroborate, **9** (0.1 g, 0.33 mmol), and Dess−Martin periodinane (0.21 g, 0.5 mmol) took place for 1 h according to the procedure described above to give **15** as a brown-green powder (0.09 g, 91%). ^{1}H NMR (500 MHz, $CDCl_3$) δ 10.56 (s, 1H), 6.28 (s, 1H), 2.63 (s, 3H), 2.61 (s, 3H), 2.25 (s, 3H), 2.17 (s, 3H); ^{13}C NMR (125 MHz, $CDCl_3$) δ 191.6, 166.6, 156.3, 146.4, 140.7, 136.9, 132.4, 125.9, 125.2, 114.3, 103.5, 15.8, 15.6, 14.0, 13.5; HRMS (ESI) for $C_{15}H_{14}N_3OBF_2$ (M^-) calcd 300.11143, found 300.11236; FTIR 976, 1059, 1316, 1549, 2220, 1714 cm^{-1}.

8-Formyl-2,6-dicyano-1,3,5,7-tetramethyl Pyrromethene Fluoroborate, 16. Reaction of 8-hydroxymethyl-2,6-dicyano-1,3,5,7-tetramethyl pyrromethene fluoroborate, **10** (0.1 g, 0.3 mmol), and Dess−Martin periodinane (0.19 g, 0.45 mmol) took place for 1.5 h according to the procedure described above to give **16** as a purple powder (0.095 g, 97%). ^{1}H NMR (500 MHz, $CDCl_3$) δ 10.59 (s, 1H), 2.73 (s, 6H), 2.36 (s, 6H); ^{13}C NMR (125 MHz, $CDCl_3$) δ 190.2, 162.4, 147.8, 140.2, 128.8, 112.8, 107.3, 14.9, 14.2; HRMS (ESI) for $C_{16}H_{13}N_4OBF_2$ (M^-) calcd 325.10777, found 325.10689; FTIR 995, 1197, 1313, 1545, 1718, 2228 cm^{-1}.

8-(N-Butyl)-methylimine-2,6-diethyl-1,3,5,7-tetramethyl Pyrromethene Fluoroborate, 20. Butylamine (0.02 g, 0.27 mmol, 1.5 equiv) and Dabco (0.12 g, 1.08 mmol, 6 equiv) were dissolved in 1 mL of dry toluene under argon. The solution was heated to 90 °C. Titanium chloride (0.27 mL of 1 M in dichloromethane, 1.5 equiv) was added dropwise to the heated reaction mixture, followed by addition of 1 mL of a toluene solution of 8-formyl-2,6-diethyl-1,3,5,7-tetramethyl pyrromethene fluoroborate, **11** (0.06 g, 0.18 mmol, 1 equiv). After 3 h of reflux the reaction mixture was cooled to room temperature. The formed precipitate was filtered and washed with dichloromethane. The solvent was evaporated under reduced pressure, and the residue was purified using flash column chromatography with hexane/ethyl acetate = 10/1. A purple powder was obtained (0.058 g, 83%); ^{1}H NMR (500 MHz, $CDCl_3$) δ 8.50 (s, 1H), 3.66−3.70 (dt, 2H), 2.49 (s, 6H), 2.33−2.37 (q, 4H), 2.01 (s, 6H), 1.72−1.77 (quintet, 2H), 1.44−1.51 (sextet, 2H), 1.01−1.04 (t, 6H), 0.96−0.99 (t, 3H); ^{13}C NMR (125 MHz, $CDCl_3$) δ 157.1, 154.8, 136.9, 134.8, 132.8, 129.9, 62.1, 31.9, 30.8, 17.1, 14.7, 13.9, 13.8, 12.6; HRMS (ESI) for $C_{22}H_{32}BF_2N_3$ (M^+) calcd 388.27301 found 388.27342; FTIR 1651, 1538, 1321, 1190, 1043, 961 cm^{-1}

8-(N-Butyl)-methylimine-2-chloro-1,3,5,7-tetramethyl Pyrromethene Fluoroborate, 21. 8-Formyl-2-chloro-1,3,5,7-tetramethyl pyrromethene fluoroborate, **13** (0.015 g, 0.05 mmol, 1 equiv), was dissolved in 1 mL of dry dichloromethane. Butylamine (0.006 g, 0.075 mmol, 1.5 equiv) was added to the solution. The reaction was left stirring under argon at room temperature for 10 h, after which the solvent was evaporated under reduced pressure. The

product was purified by column chromatography from CH_2Cl_2 to yield a purple powder (0.015 g, 85%). ^{1}H NMR (500 MHz, $CDCl_3$) δ 8.49 (s, 1H), 6.09 (s, 1H), 3.72−3.69 (dt, 2H, J = 6.1 Hz, J = 1.5 Hz), 2.54 (s, 6H), 2.11 (s, 3H), 2.09 (s, 3H), 1.78−1.72 (quintet, 2H), 1.50−1.46 (sextet, 2H), 0.99−0.97 (t, 3H, J = 7.3 Hz); ^{13}C NMR (125 MHz, $CDCl_3$) δ 159.2, 155.8, 151.1, 143.5, 136.5, 134.9, 131.4, 127.9, 122.1, 62.2, 31.9, 20.8, 16.7, 14.9, 13.9, 13.8, 12.4; MS (ESI) for $C_{18}H_{23}BClF_2N_3$ (M^-) calcd 364.16416 found 364.30; FTIR 1655, 1550, 1313, 1190, 987 cm^{-1}

8-(N-Butyl)-methylamine-2,6-diethyl-1,3,5,7-tetramethyl Pyrromethene Fluoroborate, 22. 8-(*N*-Butyl)-methylimine-2,6-diethyl-1,3,5,7-tetramethyl pyrromethene fluoroborate, **20** (0.05 g, 0.13 mmol, 1 equiv), was dissolved in dry methanol. $NaCNBH_3$ (0.012 g, 0.2 mmol, 1.5 equiv) was added to the solution, and the reaction mixture was left stirring at room temperature under argon. After 2 h the reaction mixture was condensed under reduced pressure and purified by column chromatography from CH_2Cl_2. The product was isolated as a red powder (0.048 g, 95%). ^{1}H NMR (500 MHz, $CDCl_3$) δ 3.70 (s, 2H), 2.72−2.74 (t, 2H), 2.49 (s, 6H), 2.37−2.42 (m, 10H), 1.49−1.54 (quintet, 2H), 1.35−1.41 (sextet, 2H), 1.03−1.07 (t, 6H), 0.91−0.94 (t, 3H); ^{13}C NMR (125 MHz, $CDCl_3$) δ 153.4, 136.3, 132.8, 131.8, 50.1, 45.5, 32.2, 20.5, 17.2, 14.7, 13.9, 12.5; HRMS (ESI) for $C_{22}H_{34}BF_2N_3$ (M^+) calcd 390.28866 found 390.28879; FTIR 1546, 1345, 1190, 972 cm^{-1}

8-(N-Butyl)-methylamine-2-chloro-1,3,5,7-tetramethyl Pyrromethene Fluoroborate, 23. 8-(*N*-Butyl)-methylimine-2-chloro-1,3,5,7-tetramethyl pyrromethene fluoroborate, **21** (0.01 g, 0.027 mmol, 1 equiv), was dissolved in 1 mL of dry methanol. $NaCNBH_3$ (0.005 g, 0. 81 mmol, 3 equiv) was added to the solution, and the reaction mixture was left stirring at room temperature under argon. After 2 h the reaction mixture was condensed under reduced pressure and purified by column chromatography from CH_2Cl_2. The product was isolated as red powder (0.08 g, 81%). ^{1}H NMR (500 MHz, $CDCl_3$) δ 6.11 (s, 1H), 3.92 (s, 2H), 2.72−2.75 (t, 2H, J = 7.1 Hz, J = 6.8 Hz), 2.53 (s, 6H), 2.48 (s, 3H), 2.46 (s, 3H), 1.54−1.50 (m, 2H), 1.40−1.36 (sextet, 2H), 0.94−0.91 (t, 3H, J = 7.4 Hz); ^{13}C NMR (125 MHz, $CDCl_3$) δ 157.5, 149.7, 142.9, 140.7, 134.3, 133.0, 122.6, 50.2, 45.3, 32.3, 20.5, 15.7, 14.7, 13.9, 12.5, 12.2; MS (ESI) for $C_{18}H_{25}BClF_2N_3$ (M^-) cald 367.17981 found 366.22; FTIR 1550, 1475, 1358, 1990, 980 cm^{-1}

Acknowledgment. G.C. is grateful to McGill University, the Natural Sciences and Engineering Research Council of Canada, the Canada Foundation for Innovation New Opportunities Fund, and the Centre for Self-Assembled Chemical Structures for financial assistance. K.K. is also thankful to the McGill Chemical Biology Fellowship Program and Drug Development Fellowship Program (CIHR) for a postgraduate scholarship. We are also grateful to Ms. Sayuri Friedland for assistance with extinction coefficient determinations.

Supporting Information Available: IR, ^{1}H NMR, and ^{13}C NMR spectra for compounds **1**−**16** and **20**−**23**; complete ref 30. This material is available free of charge via the Internet at http://pubs.acs.org.

JA1075663